
A. JAMES CLARK
SCHOOL OF ENGINEERING

# Cable-driven Parallel Robot Manipulator for Pick and Place Applications

Course Project Report

ENPM662-0101

Introduction to Robot Modeling

Dr. Chad Kessens

*Done By:*
Mahmoud Dahmani

*Partner:*
Saumil Shah

*Date:* 12/11/2019

# Table of Contents

1 Introduction ..... 5
2 Description of the Robot ..... 5
3 Specifications of the Robot ..... 7
4 Modeling of the Robot ..... 7
4.1 Assumptions ..... 7
4.2 Convention ..... 8
4.3 Inverse Kinematics ..... 8
4.3.1 Inverse Position Kinematics ..... 8
4.3.2 Inverse Velocity Kinematics ..... 9
4.4 Statics ..... 10
4.5 Grasping ..... 11
5 Model Validation ..... 13
5.1 Inverse Position Kinematics ..... 13
5.2 Statics and Inverse Velocity Kinematics ..... 14
5.3 Grasping ..... 15
6 Conclusion and Future Work ..... 15
Appendix ..... 17
References ..... 21

# LIST OF FIGURES

Figure 2.1: Parallel Gripper ..... 5

Figure 2.2: 8-Cable-driven Parallel Robot (Proposed System) ..... 6

Figure 2.3: 6-Cable-driven Parallel Robot ..... 6

Figure 3.1: CAD model of an 8-Cable-driven Parallel Robot ..... 7

Figure 4.2: Kinematic diagram of a CDPR ..... 9

Figure 4.3: Grasp Diagram of a Parallel Gripper ..... 12

Figure 5.1: Grasping an Object ..... 15

# LIST OF TABLES

Table 5.1: Inverse Position Kinematics Results ..... 13

Table 5.2: Statics Results ..... 14

# 1 Introduction

Processes inside big warehouses are increasingly experiencing automation. One such important task is moving heavy loads from one place to another. It takes several serial manipulators to perform it due to their small workspaces. Another alternative to cover the whole area of a warehouse, is to deploy serial manipulators on automatic guided vehicles which is a bit complex. This project proposes a simpler and a more efficient solution to the movement of heavy loads, namely a cable-driven parallel robot manipulator.

Parallel robots offer many advantages making them better suited than their serial counterparts to this kind of industrial applications. Thanks to their closed loop structure, they have faster responses and can carry heavier weights. Cable-driven parallel robots extend the notion of parallel robots by adding the properties of cables to the principles of parallel robots. In other terms, the rigid links of a parallel robot are replaced with cables under tension, thus making cable-driven parallel robots have a lighter mechanical assembly and larger workspace than conventional parallel robots.

# 2 Description of the Robot

This project aims to design and model a cable-driven parallel robot (CDPR) that carries out a pick-and-place operation inside a warehouse using a parallel gripper attached to a cubic box as an end-effector. The design of the gripper is depicted in Figure 2.1.

**Figure 2.1: Parallel Gripper**

The robot should be capable of placing the rigid object it picks at any position (x, y, z) within its 3-D workspace and at any orientation (Roll, Pitch, Yaw), and therefore it must have at least 6 degrees of freedom (DOF).

Figure 2.2 shows the design of the proposed system. The CDPR consists of 8 cables under tension. Each cable is connected to the corner of the common end-effector box through a spherical joint on one end, and to an actuator (i.e. motor) on the other end. Each cable also passes through a fixed universal joint that is implemented as the combination of a pulley with a revolute joint rotating around the vertical axis. All the joints are unactuated so the pose (position and orientation) of the end-effector is fully controlled by varying the lengths of the cables, which is achieved by rolling of the spools that hold the cables. That's why, the proposed CDPR has 8 axes (DOF) which are the cables' variable lengths ($l_i$). $l_i$ is defined as the distance from the fixed $i^{th}$ universal joint to the $i^{th}$ spherical joint attached to the end-effector; $1 \leq i \leq 8$.

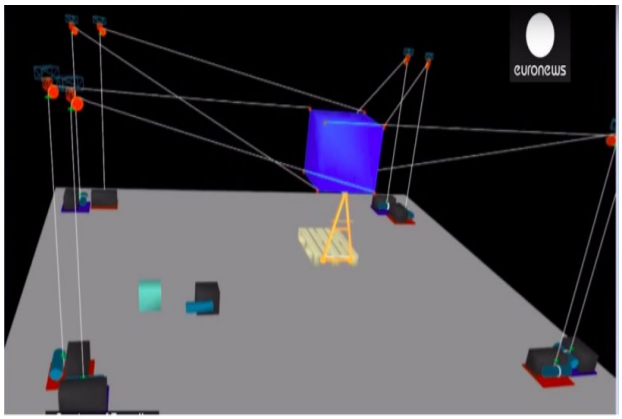


**Figure 2.2: 8-Cable-driven Parallel Robot (Proposed System)**

It should be noted that 6 cables are enough for the design of the CDPR as shown in Figure 2.3. Cables can only execute a pulling action and they cannot exert a push. As a result, the end-effector motion will be slow and subject to vibrations. However, making the CDPR kinematically redundant by introducing 2 additional cables resolves the issue by ensuring a better tension distribution. Hence, the end-effector of the 8-DOF CDPR will move at a higher speed with less vibrations.

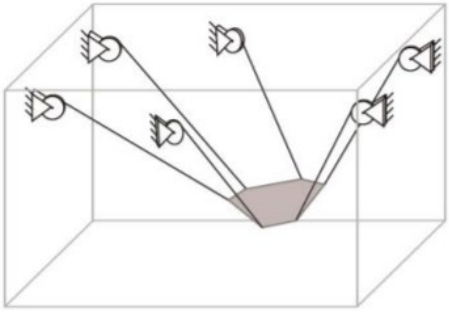

**Figure 2.3: 6-Cable-driven Parallel Robot**

# 3 Specifications of the Robot

SolidWorks is used to design a 3D CAD model of an 8-cable-driven parallel robot that has a cubic workspace of side 3.5m and a cubic end-effector box of side of 0.6m as illustrated in Figure 3.1. The gripper is modeled as two parallel rectangular fingers of dimensions 0.6m x 0.2m x 0.1m.

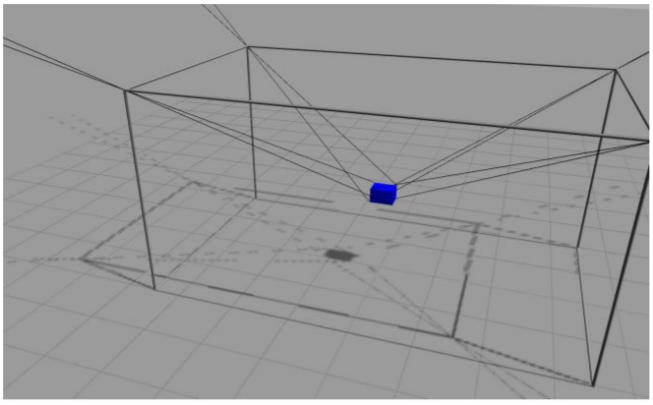

**Figure 3.1: CAD model of an 8-Cable-driven Parallel Robot**

The fixed universal joints' positions are defined relative to the world frame as follows:

$$U = [\vec{u}_1 \quad \vec{u}_2 \quad \vec{u}_3 \quad \vec{u}_4 \quad \vec{u}_5 \quad \vec{u}_6 \quad \vec{u}_7 \quad \vec{u}_8]$$

$$U = \begin{bmatrix} -3.5 & -3.5 & 3.5 & 3.5 & -3.5 & -3.5 & 3.5 & 3.5 \\ -3.5 & -3.5 & -3.5 & -3.5 & 3.5 & 3.5 & 3.5 & 3.5 \\ 3.5 & 3.5 & 3.5 & 3.5 & 3.5 & 3.5 & 3.5 & 3.5 \end{bmatrix}$$

The spherical joints' positions are defined relative to the end-effector frame as follows:

$$S = [\vec{s}_1 \quad \vec{s}_2 \quad \vec{s}_3 \quad \vec{s}_4 \quad \vec{s}_5 \quad \vec{s}_6 \quad \vec{s}_7 \quad \vec{s}_8]$$

$$S = \begin{bmatrix} 0.3 & -0.3 & -0.3 & 0.3 & -0.3 & 0.3 & 0.3 & -0.3 \\ -0.3 & 0.3 & -0.3 & 0.3 & -0.3 & 0.3 & -0.3 & 0.3 \\ -0.3 & 0.3 & 0.3 & -0.3 & -0.3 & 0.3 & 0.3 & -0.3 \end{bmatrix}$$

# 4 Modeling of the Robot

## *4.1 Assumptions*

- The entire warehouse structure is rigid.
- The robot utilizes its parallel gripper to grasp a metallic cubic object that has a rigid rectangular handle and whose pose is known.
- All cables are massless, rigid and don't interfere with each other.
- The cables whose lengths are variable are modeled as prismatic joints with displacements $\vec{l}_i$ in the direction of the cables' tensions (i.e. pointing to the spherical joints).
- All joints are massless and frictionless.

- There is no mechanical power loss in the robot.
- All the motors need not generate any torques for the robot to support itself against gravity.
- All the motors have access to any required torque.
- The workspace is obstacle-free which eliminates the need for path planning.
- Two universal joints are fixed at every upper corner of the workspace as depicted in Figure 3.1. This assumption simplifies the simulation and once the correctness of kinematics modeling is verified, it can be readily manipulated to apply the results to the real world.

## *4.2 Convention*

- The superscript of a vector denotes the reference frame it was expressed in, such that the 0-frame is the base frame and the n-frame is the tool frame.
- The symbol S denotes the Skew-symmetric matrix Operator defined as:

$$S(\vec{v}) = \begin{bmatrix} 0 & -v3 & v2 \\ v3 & 0 & -v1 \\ -v2 & v1 & 0 \end{bmatrix}$$

## *4.3 Inverse Kinematics*

### *4.3.1 Inverse Position Kinematics*

Solving the Inverse Position Kinematics serves the purpose of controlling the pose of the end-effector.

Problem Statement

Given a desired position $\vec{o}_d = \vec{o}_d^0 = [x_d\ y_d\ z_d]^T$ and a desired orientation $R_d = R_n^0(Roll_d, Pitch_d, Yaw_d)$ of the end-effector, the CDPR configuration $\vec{q} = \vec{l} = [l_1\ l_2\ l_3\ l_4\ l_5\ l_6\ l_7\ l_8]^T$ is computed geometrically.

The desired end-effector pose can be alternatively given as the homogeneous transformation $T_d = T_n^0 = \begin{bmatrix} R_d & \vec{o}_d \\ 0_{1x3} & 1 \end{bmatrix}$, such that $R_d$ is the 3x3 rotation matrix.

Solution

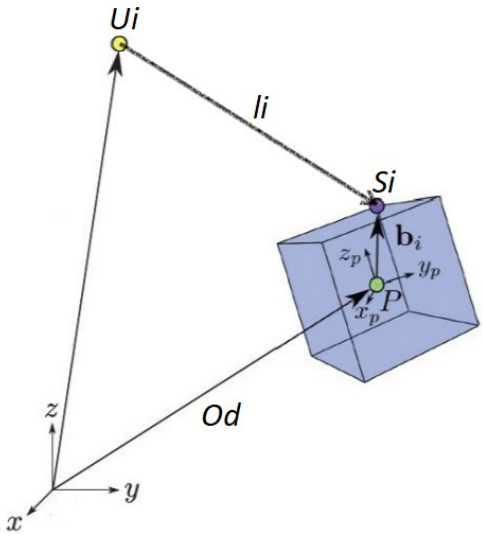


**Figure 4.2: Kinematic diagram of a CDPR**

Let $\vec{l}_i = \vec{l}_i^0 = [l_{i_x}\ l_{i_y}\ l_{i_z}]^T$ be the cable's length vector from the fixed i[th] universal joint to the moving i[th] spherical joint.

Knowing the positions of the universal joints $\vec{u}_i = \vec{u}_i^0 = [u_{i_x}\ u_{i_y}\ u_{i_z}]^T$ and the positions of the spherical joints $\vec{s}_i = \vec{s}_i^n = [s_{i_x}\ s_{i_y}\ s_{i_z}]^T$, we see from Figure 4.2,

$$\vec{l}_i = \vec{s}_i^0 - \vec{u}_i^0 = (R_d\ \vec{s}_i + \vec{o}_d) - \vec{u}_i$$

The CDPR configuration is:

$$q_i = l_i = \|\vec{l}_i\| = \sqrt{\vec{l}_i \,.\, \vec{l}_i} = \sqrt{\vec{l}_i^{\,T}\ \vec{l}_i}\ ;\ 1 \le i \le 8$$

### *4.3.2 Inverse Velocity Kinematics*

Solving the Inverse Position Kinematics serves the purpose of controlling the twist (linear and angular velocity) of the end-effector.

Problem Statement

Given desired end-effector velocities $\vec{\xi}_d = \vec{\xi}_d^0 = [\vec{v}_d\ \vec{\omega}_d]^T$, the speed of the cables $\dot{\vec{q}} = \dot{\vec{l}} = [\dot{l}_1\ \dot{l}_2\ \dot{l}_3\ \dot{l}_4\ \dot{l}_5\ \dot{l}_6\ \dot{l}_7\ \dot{l}_8]^T$ is determined by deriving the manipulator inverse Jacobian $J_{inv} = J_{inv}(q)$ which satisfies the equation $\dot{\vec{q}} = J_{inv}(q)\ \vec{\xi}_d$.

Solution

$$\dot{q}_i = \dot{l}_i = \frac{\frac{d}{dt}(\vec{l}_i \,.\, \vec{l}_i)}{2\sqrt{\vec{l}_i \,.\, \vec{l}_i}} = \frac{\dot{\vec{l}}_i \,.\, \vec{l}_i + \vec{l}_i \,.\, \dot{\vec{l}}_i}{2\sqrt{l_i^2}} = \frac{\dot{\vec{l}}_i \,.\, \vec{l}_i + \vec{l}_i \,.\, \dot{\vec{l}}_i}{2l_i} = \frac{\vec{l}_i \,.\, \dot{\vec{l}}_i}{l_i} = \left(\frac{\vec{l}_i}{l_i}\right).\dot{\vec{l}}_i = \hat{l}_i \,.\, \dot{\vec{l}}_i = \hat{l}_i \,.\, (\dot{R}_d \vec{s}_i + \dot{\vec{o}}_d)$$

where $\hat{l}_i = \frac{\vec{l}_i}{l_i}$ is the unit vector in the direction of $\vec{l}_i$.

$$\dot{q}_i = \hat{l}_i \,.\, (S(\vec{\omega}_d)R_d\vec{s}_i + \vec{v}_d) = \hat{l}_i \,.\, (\vec{\omega}_d \times R_d\vec{s}_i) + \hat{l}_i \,.\, \vec{v}_d = \vec{\omega}_d \,.\, (R_d\vec{s}_i \times \hat{l}_i) + \hat{l}_i \,.\, \vec{v}_d$$

$$\dot{q}_i = \hat{l}_i \,.\, \vec{v}_d + (R_d\vec{s}_i \times \hat{l}_i) \,.\, \vec{\omega}_d = [\hat{l}_i \; R_d\vec{s}_i \times \hat{l}_i] \,.\, [\vec{v}_d \; \vec{\omega}_d] \;;\; 1 \le i \le 8$$

$$\dot{\vec{q}} = \begin{bmatrix} \hat{l}_1^{\,T} & (R_d\vec{s}_1 \times \hat{l}_1)^T \\ \vdots & \vdots \\ \hat{l}_8^{\,T} & (R_d\vec{s}_8 \times \hat{l}_8)^T \end{bmatrix} \begin{bmatrix} \vec{v}_d \\ \vec{\omega}_d \end{bmatrix}$$

$$\dot{\vec{q}} = \dot{\vec{l}} = \begin{bmatrix} \hat{l}_1^{\,T} & (R_d\vec{s}_1 \times \hat{l}_1)^T \\ \vdots & \vdots \\ \hat{l}_8^{\,T} & (R_d\vec{s}_8 \times \hat{l}_8)^T \end{bmatrix} \vec{\xi}_d$$

$$\Rightarrow J_{inv} = \begin{bmatrix} \hat{l}_1^{\,T} & (R_d\vec{s}_1 \times \hat{l}_1)^T \\ \vdots & \vdots \\ \hat{l}_8^{\,T} & (R_d\vec{s}_8 \times \hat{l}_8)^T \end{bmatrix}$$

## *4.4 Statics*

Solving the Statics serves the purpose of controlling the forces and moments applied by the end-effector to grasp an object.

Problem Statement

Given a desired wrench $\vec{F}_d = \vec{F}_d^0 = [\vec{f}_d \; \vec{m}_d]^T$ at the end-effector, the tension distribution $\vec{\tau} = [\tau_1 \; \tau_2 \; \tau_3 \; \tau_4 \; \tau_5 \; \tau_6 \; \tau_7 \; \tau_8]^T$ in the cables is determined using the principle of conservation of power:

*power at the joints = power to move the robot + power at the end-effector*

Solution

Suppose the robot is at rest (i.e. static equilibrium)

$$\Rightarrow \text{ power to move the robot} = 0$$

$$\Rightarrow \text{ power at the joints } = \text{ power at the end effector}$$

$$\vec{\tau} \,.\, \dot{\vec{q}} = \vec{F}_d^0 \,.\, \vec{\xi}_d^0$$

$$\dot{\vec{q}}^T \vec{\tau} = \vec{\xi}_d^{0\,T} \vec{F}_d^0$$

$$(J_{inv}\, \vec{\xi}_d^0)^T \vec{\tau} = \vec{\xi}_d^{0\,T} \vec{F}_d$$

$$\vec{\xi}_d^{0\,T} J_{inv}^{\,T} \vec{\tau} = \vec{\xi}_d^{0\,T} \vec{F}_d$$

$$\Rightarrow J_{inv}^{\,T} \vec{\tau} = \vec{F}_d$$

$$\Rightarrow \vec{\tau} = (\mathrm{J}_{inv}{}^{\mathrm{T}})^{\dagger}\, \vec{\mathrm{F}}_{\mathrm{d}}$$

where $(\mathrm{J}_{inv}{}^{\mathrm{T}})^{\dagger}$ is the Moore-Penrose Pseudoinverse of $\mathrm{J}_{inv}{}^{\mathrm{T}}$.

Alternative Solution

The cables' tensions $\tau$ can also be obtained by formulating the problem as a quadratic mathematical program as follows:

$$\min \ \|\vec{\tau}\|^2$$

$$\text{subject to} \begin{cases} \mathrm{J}_{inv}{}^{\mathrm{T}}\, \vec{\tau} = \vec{\mathrm{F}}_{\mathrm{d}} \\ \tau_{\mathrm{i}} \geq 0;\ 1 \leq \mathrm{i} \leq 8 \end{cases}$$

This approach is interesting because it yields the minimum Euclidean norm solution, thus the most power efficient tension distribution. Furthermore, this constrained optimization formulation of the statics ensures that the tensions are non-negative which captures the inherent inability of cables to work in compression.

### *4.5 Grasping*

Solving the grasping problem serves the purpose of determining the set of contact forces and torques exerted by the end-effector (gripper) to resist the external wrench applied by the object to be held.

Problem Statement

Given an object wrench $\vec{\mathrm{F}}_{\mathrm{o}} = \vec{\mathrm{F}}_{\mathrm{o}}^{\mathrm{n}} = [\vec{\mathrm{f}}_{\mathrm{o}}\ \vec{\mathrm{m}}_{\mathrm{o}}]^{\mathrm{T}}$ measured by a 6-axis force-torque sensor placed at the end-effector, the gripper must apply a number of contact wrenches $\vec{\mathrm{F}}_{\mathrm{c}_i}$ that generate a minimum net wrench $\vec{\mathrm{F}}_{\mathrm{g}} = \vec{\mathrm{F}}_{\mathrm{g}}^{\mathrm{n}} = -\vec{\mathrm{F}}_{\mathrm{o}}$. Note that grasping can be done harder than necessary because the object is assumed to be rigid.

Solution

The interaction between the parallel gripper and the object results in a rectangular contact area on either side of the object. To ensure a firm grip of the object, 4 contact wrenches are assumed to be applied at the vertices of both contact areas, amounting to 8 contact wrenches $\vec{\mathrm{F}}_{\mathrm{c}_i}$ in total; $1 \leq \mathrm{i} \leq 8$. This is illustrated in Figure 4.3.

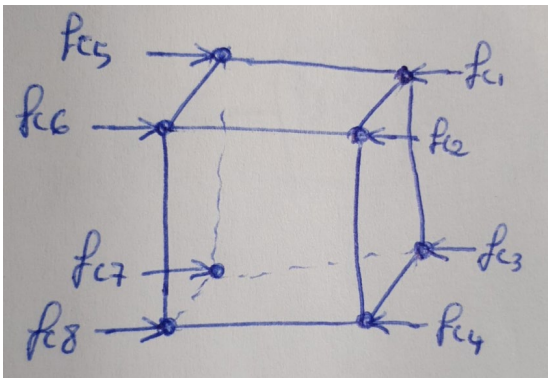


**Figure 4.3: Grasp Diagram of a Parallel Gripper**

The soft-finger contact model is adopted

$$\Rightarrow \begin{cases} \text{wrench basis} = B_{c_i} = \begin{bmatrix} 1 & 0 & 0 & 0 \\ 0 & 1 & 0 & 0 \\ 0 & 0 & 1 & 0 \\ 0 & 0 & 0 & 0 \\ 0 & 0 & 0 & 0 \\ 0 & 0 & 0 & 1 \end{bmatrix} \\ \text{contact force} = \vec{f}_{c_i} = \left[f_{i_1}\ f_{i_2}\ f_{i_3}\ f_{i_4}\right]^T \in FC_{c_i}; \\ FC_{c_i} = \left\{\vec{f} \in \mathbb{R}^4 : \sqrt{{f_1}^2 + {f_2}^2} \leq \mu f_3, f_3 \geq 0, |f_4| \leq \gamma f_3\right\} \end{cases}$$

where the static coefficient of friction $\mu = 1$ and the coefficient of torsional friction $\gamma = 1$.

The contact map $G_i = Ad^T\left(T_{c_i}^{o\,-1}\right) B_{c_i} = \begin{bmatrix} R_{c_i}^o & 0_{3x3} \\ S(\vec{o}_{c_i})R_{c_i}^o & R_{c_i}^o \end{bmatrix} \begin{bmatrix} 1 & 0 & 0 & 0 \\ 0 & 1 & 0 & 0 \\ 0 & 0 & 1 & 0 \\ 0 & 0 & 0 & 0 \\ 0 & 0 & 0 & 0 \\ 0 & 0 & 0 & 1 \end{bmatrix}$

Let $\begin{cases} \vec{f}_c = [{\vec{f}_{c_1}}^T\ {\vec{f}_{c_2}}^T \dots {\vec{f}_{c_8}}^T]^T \in FC;\ FC = FC_{c_1} \times FC_{c_2} \times \dots \times FC_{c_8} \\ G = [G_1\ G_2 \dots G_8] \end{cases}$

$$\vec{F}_g = G\,\vec{f}_c$$

$$\Rightarrow \vec{f}_c = G^{\dagger}\,\vec{F}_g$$

where $G^{\dagger}$ is the Moore-Penrose Pseudoinverse of G.

<u>Alternative Solution</u>

The contact forces $\vec{f}_c$ can be alternatively computed by formulating the problem as a quadratic mathematical program as follows:

$$\min \left\|\vec{f}_c\right\|^2$$

$$\text{subject to} \begin{cases} \vec{F}_g = G\,\vec{f}_c \\ f_{i_3} \geq 0;\ 1 \leq i \leq 8 \end{cases}$$

This method has the advantage of fulfilling the condition that a parallel gripper can only exert pushing forces in the direction of action.

# 5 Model Validation

The validation of the mathematical models derived in the previous section was done by means of a Gazebo simulation of the 8-cable-driven parallel robot. Videos of the robot simulation can be found at the following GitHub repository link: https://github.com/SaumilShah66/CDPR-Robot-modelling-project.git

## *5.1 Inverse Position Kinematics*

The inverse position kinematics is validated by verifying that the discrepancy between the theoretical and simulated cable length results for 4 arbitrary end-effector poses is negligible. According to Table 5.1, the absolute value of the maximum relative error is 1.8% and hence the model is valid.

**Table 5.1: Inverse Position Kinematics Results**

| Example | Cable Length (m) | Theoretical | Simulation | Error (%) |
|---|---|---|---|---|
| 1 | L1 | 5.43323 | 5.42123 | -0.2209 |
| | L2 | 5.70263 | 5.72631 | 0.41525 |
| | L3 | 5.70263 | 5.61263 | -1.5782 |
| | L4 | 5.43323 | 5.42311 | -0.1863 |
| | L5 | 5.43323 | 5.33231 | -1.8575 |
| | L6 | 5.70263 | 5.7631 | 1.06039 |
| | L7 | 5.70263 | 5.7031 | 0.00824 |
| | L8 | 5.43323 | 5.40829 | -0.459 |
| 2 | L1 | 6.74685 | 6.85112 | 1.54546 |
| | L2 | 6.96563 | 6.92991 | -0.5128 |
| | L3 | 5.97662 | 5.9119 | -1.0829 |
| | L4 | 5.50636 | 5.516 | 0.17507 |
| | L5 | 5.72014 | 5.71399 | -0.1075 |
| | L6 | 5.77235 | 5.73479 | -0.6507 |
| | L7 | 4.5299 | 4.54066 | 0.23753 |
| | L8 | 4.18569 | 4.1569 | -0.6878 |
| 3 | L1 | 6.677 | 6.69782 | 0.31182 |
| | L2 | 7.03262 | 7.02169 | -0.1554 |
| | L3 | 6.03582 | 6.0274 | -0.1395 |
| | L4 | 5.44141 | 5.44068 | -0.0134 |
| | L5 | 5.65442 | 5.64184 | -0.2225 |
| | L6 | 5.83674 | 5.81942 | -0.2967 |
| | L7 | 4.58704 | 4.59409 | 0.15369 |
| | L8 | 4.12299 | 4.12911 | 0.14844 |

| | | | | |
|---|---|---|---|---|
| **4** | L1 | 6.63673 | 6.64264 | 0.08905 |
| | L2 | 7.07063 | 7.06338 | -0.1025 |
| | L3 | 6.08699 | 6.09858 | 0.19041 |
| | L4 | 5.38411 | 5.37066 | -0.2498 |
| | L5 | 5.71015 | 5.71496 | 0.08424 |
| | L6 | 5.78223 | 5.78306 | 0.01435 |
| | L7 | 4.53163 | 4.51634 | -0.3374 |
| | L8 | 4.18381 | 4.1913 | 0.17902 |

## *5.2 Statics and Inverse Velocity Kinematics*

The statics and inverse velocity kinematics can be validated at once because both of their solutions are represented as a given vector multiplied by a function of the same Jacobian matrix. The statics model is validated by showing that the discrepancy between the theoretical and simulated cable tension results for 4 arbitrary end-effector wrenches is negligible. According to Table 5.2, the absolute value of the maximum relative error is 0.9% and hence the model is accurate. Consequently, the inverse velocity kinematics is valid as well.

**Table 5.2: Statics Results**

| Example | Cable Tension (N) | Theoretical | Simulation | Error (%) |
|---|---|---|---|---|
| **1** | T1 | 418.41 | 419.14338 | 0.17528 |
| | T2 | 398.606 | 399.34248 | 0.18477 |
| | T3 | 398.606 | 399.34248 | 0.18477 |
| | T4 | 418.41 | 419.14338 | 0.17528 |
| | T5 | 418.41 | 419.14338 | 0.17528 |
| | T6 | 398.606 | 399.34248 | 0.18477 |
| | T7 | 398.606 | 399.34248 | 0.18477 |
| | T8 | 418.41 | 419.14338 | 0.17528 |
| **2** | T1 | 329.766 | 329.33196 | -0.1316 |
| | T2 | 326.958 | 326.69129 | -0.0816 |
| | T3 | 316.6973 | 316.49109 | -0.0651 |
| | T4 | 339.465 | 339.06603 | -0.1175 |
| | T5 | 483.254 | 483.0292 | -0.0465 |
| | T6 | 462.497 | 462.08194 | -0.0897 |
| | T7 | 454.726 | 454.39369 | -0.0731 |
| | T8 | 490.36 | 490.16884 | -0.039 |
| **3** | T1 | 280.269 | 278.74223 | -0.5448 |
| | T2 | 276.355 | 275.45646 | -0.3251 |
| | T3 | 353.167 | 353.35737 | 0.0539 |
| | T4 | 389.811 | 388.37995 | -0.3671 |
| | T5 | 375.858 | 375.10563 | -0.2002 |

| | | | | |
|---|---|---|---|---|
| | T6 | 368.9 | 367.07618 | -0.4944 |
| | T7 | 523.4 | 522.48884 | -0.1741 |
| | T8 | 562.426 | 561.78379 | -0.1142 |
| 4 | T1 | 624.071 | 623.07271 | -0.16 |
| | T2 | 578.497 | 576.75787 | -0.3006 |
| | T3 | 432.035 | 428.19852 | -0.888 |
| | T4 | 438.654 | 437.29356 | -0.3101 |
| | T5 | 400.364 | 397.51382 | -0.7119 |
| | T6 | 359.475 | 359.93522 | 0.12803 |
| | T7 | 308.288 | 306.77284 | -0.4915 |
| | T8 | 306.769 | 303.96828 | -0.913 |

### *5.3 Grasping*

Grasping was tested differently. An object of mass 1 Kg was used to validate the contact forces required to resist the wrench applied by a load's weight. Two experiments were conducted. The first was the application of a total force of 6N (by computing the corresponding 4 contact forces) at both gripper fingers. The object was successfully grasped as shown in Figure 5.1. The Second was applying a total force of 5N (by computing the corresponding 4 contact forces) at both gripper fingers. The object slips and could not be picked up. The outcomes of these two experiments are demonstrated in the videos available at the link above.

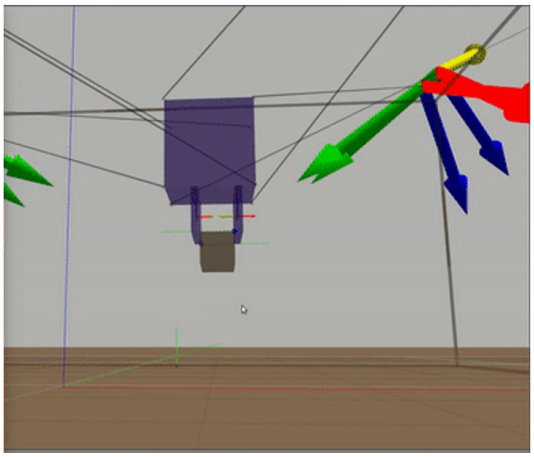

**Figure 5.1: Grasping an Object**

# 6 Conclusion and Future Work

In this report, many aspects of an 8-cable-driven parallel robot (8-CDPR) have been modeled, namely inverse position kinematics, inverse velocity kinematics (although it is not required according to the proposal), statics and grasping with a parallel gripper. A simulation of the robot was performed to help validate the mathematical models that were derived.

Furthermore, the simulation served as evidence to the stability of the movement of the redundantly restrained 8-CDPR. In conclusion, 8-cable-driven parallel robots are well suited to moving heavy loads form one place to another inside big warehouses.

The next step in studying cable-driven parallel robots is to model and simulate their dynamics. Another possibility for future improvement is to assume that the environment contains obstacles and accordingly implement path planning and trajectory generation.

# Appendix

The following Matlab script solves the inverse position kinematics, statics and grasping problems of an 8-cable-driven parallel robot.

```
clear all
clc

% 1. CDPR Geometry Setup
% 1.1. Joints' Positions
u = [-3.5 -3.5 3.5 3.5 -3.5 -3.5 3.5 3.5;
     -3.5 -3.5 -3.5 -3.5 3.5 3.5 3.5 3.5;
     3.5 3.5 3.5 3.5 3.5 3.5 3.5 3.5];

s = [0.3 -0.3 -0.3 0.3 -0.3 0.3 0.3 -0.3;
     -0.3 0.3 -0.3 0.3 -0.3 0.3 -0.3 0.3;
     -0.3 0.3 0.3 -0.3 -0.3 0.3 0.3 -0.3];

% 1.2. Define Contact Forces' Frames here
oc1 = rand(3,1);
Rc1 = rand(3,3);
oc2 = rand(3,1);
Rc2 = rand(3,3);
oc3 = rand(3,1);
Rc3 = rand(3,3);
oc4 = rand(3,1);
Rc4 = rand(3,3);
oc5 = rand(3,1);
Rc5 = rand(3,3);
oc6 = rand(3,1);
Rc6 = rand(3,3);
oc7 = rand(3,1);
Rc7 = rand(3,3);
oc8 = rand(3,1);
Rc8 = rand(3,3);

% 2. Inverse Kinematics
% Specify Inputs here
od = [0,0,1]';
Rd = [1,0,0;
      0,1,0;
      0,0,1];
```

```
% Solution
l1 = Rd*s(:,1) + od - u(:,1);
l2 = Rd*s(:,2) + od - u(:,2);
l3 = Rd*s(:,3) + od - u(:,3);
l4 = Rd*s(:,4) + od - u(:,4);
l5 = Rd*s(:,5) + od - u(:,5);
l6 = Rd*s(:,6) + od - u(:,6);
l7 = Rd*s(:,7) + od - u(:,7);
l8 = Rd*s(:,8) + od - u(:,8);

q = [norm(l1) norm(l2) norm(l3) norm(l4) norm(l5)
norm(l6) norm(l7) norm(l8)]'

% 3. Statics
% Specify Inputs here
Fd = [0,0,-150*9.8,0,0,0]';

% Solution
Jinv = [(l1/norm(l1))'
cross(Rd*s(:,1),l1/norm(l1))';
        (l2/norm(l2))'
cross(Rd*s(:,2),l2/norm(l2))';
        (l3/norm(l3))'
cross(Rd*s(:,3),l3/norm(l3))';
        (l4/norm(l4))'
cross(Rd*s(:,4),l4/norm(l4))';
        (l5/norm(l5))'
cross(Rd*s(:,5),l5/norm(l5))';
        (l6/norm(l6))'
cross(Rd*s(:,6),l6/norm(l6))';
        (l7/norm(l7))'
cross(Rd*s(:,7),l7/norm(l7))';
        (l8/norm(l8))'
cross(Rd*s(:,8),l8/norm(l8))'];

% Method 1 (pseudo-inverse)
T_1 = pinv(Jinv')*Fd

% Method 2 (linear optimization)
f = ones(8,1);
A = [];
```

```
b = [];
Aeq = Jinv';
beq = Fd;
lb = zeros(8,1);
ub = inf*ones(8,1);

T_2 = linprog(f,A,b,Aeq,beq,lb,ub)

% 4. Grasping
% Specify Inputs here
Fg = rand(6,1);

% Solution
Bc = [eye(6,3) [0 0 0 0 0 1]'];
G1 = AdT(Rc1,oc1)*Bc;
G2 = AdT(Rc2,oc2)*Bc;
G3 = AdT(Rc3,oc3)*Bc;
G4 = AdT(Rc4,oc4)*Bc;
G5 = AdT(Rc5,oc5)*Bc;
G6 = AdT(Rc6,oc6)*Bc;
G7 = AdT(Rc7,oc7)*Bc;
G8 = AdT(Rc8,oc8)*Bc;
G = [G1 G2 G3 G4 G5 G6 G7 G8];

% Method 1 (pseudo-inverse)
fc_1 = pinv(G)*Fg

% Method 2 (linear optimization)
f = ones(32,1);
A = [];
b = [];
Aeq = G;
beq = Fg;
lb = [-inf -inf 0 -inf, -inf -inf 0 -inf, -inf -
inf 0 -inf, -inf -inf 0 -inf, -inf -inf 0 -inf, -
inf -inf 0 -inf, -inf -inf 0 -inf, -inf -inf 0 -
inf]';
ub = inf*ones(32,1);

fc_2 = linprog(f,A,b,Aeq,beq,lb,ub)

function V = Skew(v)
```

```
% Skew-symmetric matrix Operator
V = [0 -v(3) v(2);
     v(3) 0 -v(1);
     -v(2) v(1) 0];
end

function Y = AdT(R,o)
% Adjoint matrix Operator
Y = [R zeros(3,3); Skew(o)*R R];
end
```

# References

[1] Okoli, Franklin & Lang, Yuchuan & Kermorgant, Olivier & Caro, Stéphane. (2019). Cable-Driven Parallel Robot Simulation Using Gazebo and ROS. 10.1007/978-3-319-78963-7_37.